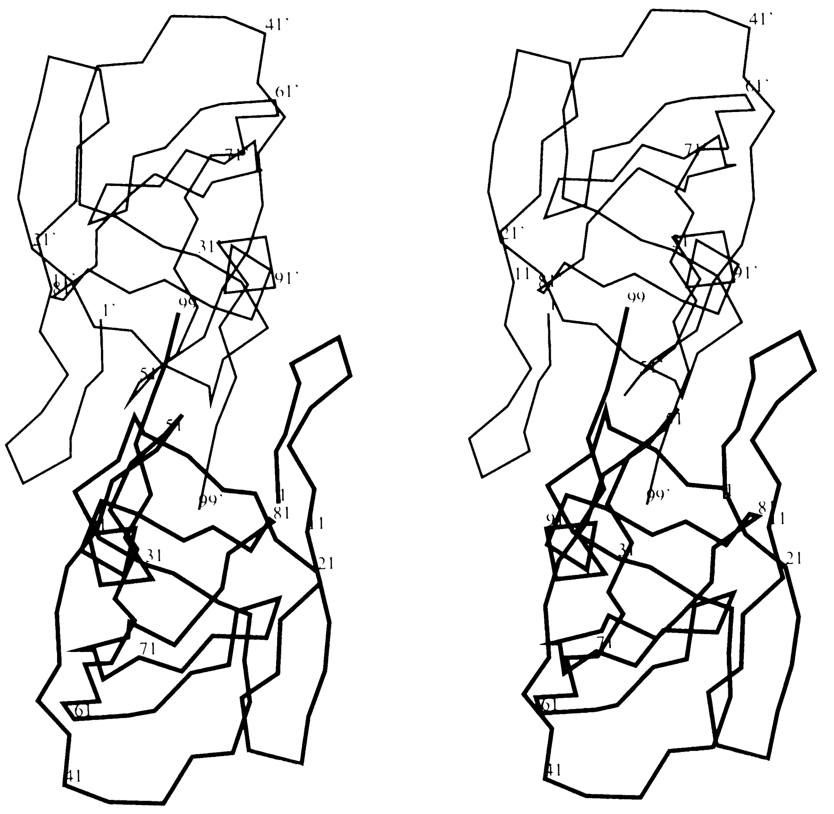

Fig. 6. A view of the Cα backbone tracing of the fully refined model of the HIV-1 protease dimer, in an orientation emphasizing the interactions in the dimer interface. The full set of atomic parameters for this model, including both the main chain and side chain atoms, has been deposited with the Brookhaven Protein Data Bank (set 3HVP).

We suggest that only intermolecular catalysis is responsible for the release of the protease in both RSV and HIV-1.

Comparison with previously proposed models of HIV-1 PR. This experimentally determined structure of HIV-1 PR has been compared with the results of the two previous modeling efforts. The superposition of the Cα atoms onto the atomic coordinates of Pearl and Taylor (*4*) yielded an rms deviation of 2.6 Å for 87 atom pairs. In a number of places the residues were shifted by one or two positions, but the general agreement was remarkably good, considering that the model was based on distant similarities to nonviral, pepsin-like proteases.

A comparison with the model of Weber *et al.* (*16*), which was based on the closely related RSV protease, yielded an rms deviation of 1.3 Å for 82 Cα atoms. In this comparison residues 1 to 6 in the refined model are shifted by two positions toward the NH_2-terminus. Deviations along the flap (residues 43 to 58) were as large as 7 Å because the flat was originally modeled in a position close to the active site as observed in a rhizopuspepsin-inhibitor complex (*35*). The location of the active site and substrate binding residues, however, was predicted quite accurately in the model of Weber *et al.* (*16*). In particular, the significance of mutations at Arg^{87} and Asn^{88} was correctly understood from that model, whereas it was not obvious from the structure reported by Navia *et al.* (*1*). Arg^{87} is located in the helix and forms an ionic interaction with Asp^{29} near the catalytic site. This is consistent with the results of mutations of Arg^{87} or Asn^{88} that produce inactive protease (*36*). Detailed modeling of inhibitor complexes based on our structure should help explain the observed differences in specificity between the RSV and HIV proteases, and can be used to design better inhibitors.

Potential applications. Our results confirm that a number of conserved features of the three-dimensional structure of aspartic proteases are also conserved in the retroviral enzymes and reinforces the notion that modeling of unknown structures based on the structures of related proteins can often give accurate results. A chemically synthesized protein can crystallize isomorphously with the protein obtained from living cells and can fold correctly without being exposed to a ribosome. The coordinates of the HIV-1 PR provided in this study will be useful in rational drug design. The information on side chain positions should allow more systematic investigations of the mechanism of this important enzyme to be made, especially with respect to design of specific inhibitors for use as potential therapeutics against AIDS. Furthermore, drugs could be designed including drugs that interfere with the dimerization and hence inactivate the enzyme through an alternative mechanism. It should be noted that one of the terminal strands contains a free Cys residue, thus suggesting a site of covalent attachment for a compound designed along these lines.

REFERENCES AND NOTES

1. M. A. Navia *et al.*, *Nature* **337**, 615 (1989).
2. N. E. Kohl *et al.*, *Proc. Natl. Acad. Sci. U.S.A.* **85**, 4686 (1988).
3. H. Toh, M. Ono, K. Saigo, T. Miyata, *Nature* **315**, 691 (1985).
4. L. Pearl and W. Taylor, *ibid.* **329**, 351 (1987).
5. J. Schneider and S. B. H. Kent, *Cell* **54**, 363 (1988).
6. J. Hansen, S. Billich, T. Schulze, S. Sukrow, K. Moelling, *EMBO J.* **7**, 1785 (1988).
7. S. Seelmeier, H. Schmidt, V. Turk, K. von der Helm, *Proc. Natl. Acad. Sci. U.S.A.* **85**, 6612 (1988).
8. P. L. Darke *et al.*, *J. Biol. Chem.* **264**, 2307 (1989).
9. A. D. Richards, R. Roberts, B. M. Dunn, M. C. Graves, J. Kay, *FEBS Lett.* **247**, 113 (1989).
10. S. F. J. Le Grice *et al.*, *EMBO J.* **7**, 2547 (1988).
11. D. D. Loeb, C. A. Hutchison, M. H. Edgell, W. G. Farmerie, R. Swanstrom, *J. Virol.* **63**, 111 (1989).
12. T. D. Meek *et al.*, *Proc. Natl. Acad. Sci. U.S.A.* **86**, 1841 (1989).
13. M. Miller, M. Jaskólski, J. K. M. Rao, J. Leis, A. Wlodawer, *Nature* **337**, 576 (1989).
14. M. N. G. James and A. R. Sielecki, in *Biological Macromolecules and Assemblies*, F. A. Jurnak and A. McPherson, Eds. (Wiley, New York, 1987), pp. 413–482.
15. T. L. Blundell and L. Pearl, *Nature* **337**, 596 (1989).
16. I. T. Weber *et al.*, *Science* **243**, 928 (1989).
17. The following side chain protection was used: Asp and Glu, benzyl-protected carboxyl group (OBz); Asn, Gln, and Met, unprotected; Lys, dichlorobenzyloxy-

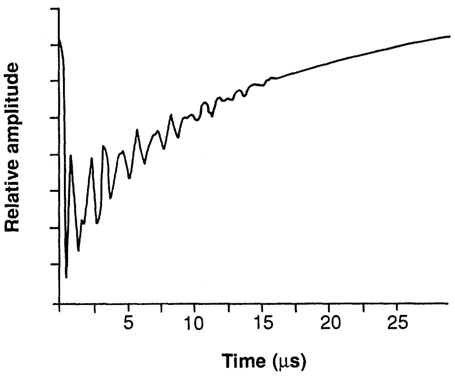

Fig. 2. An example of the transient electric field produced by a sulfur discharge during a laboratory simulation. This "signature" is similar to those produced by discharges on spacecraft dielectrics (*7*).

Discharges were recorded during all exposures. An example of the transient electric field that was produced by a sulfur discharge is shown in Fig. 2 and is generally similar to signals that are produced by discharges on spacecraft dielectrics (7). Visual observations confirmed the presence of discharges in only about half of the cases; however, this was a strong function of how well the eyes of the observers had become dark-adapted. The visible morphology of the discharges varied from event to event. On some occasions, a flash would light up the entire surface; in other cases, lightning-like patterns would appear. When the exposed surface was grounded, most of the visible discharges occurred where there was contact between the sulfur and the grounding tape. Several times, flashes covering the whole surface occurred after the electron beam was turned off.

At this stage, we have evidence that discharge phenomena do occur on natural sulfur under conditions that are similar to those expected on the surface of Io (*4*). Our simulation of Io would be more accurate if we had used samples at colder temperatures and a broader range of particle energies. Nevertheless, we expect that colder surfaces and more energetic particles will produce more frequent or stronger discharges, or both; hence, our initial simulation of the surface of Io appears valid.

The presence of surface discharges on natural dielectrics could be significant for a variety of reasons. In spacecraft, surface discharges produce localized melting and boil-off of the atoms and molecules (neutral and ionized) of the constituent material (*8*) (Fig. 3), and there can also be nonequilibrium chemical reactions and emissions of volatile species (*9*). Among the types of damage reported on polymer surfaces are subsurface tunnels, grooves, and pits caused by surface eruptions (*10, 11*). Quartz surfaces exhibit edge chipping (*12*) and other mechanical effects.

In the case of Io, surface discharges may provide a source of ions close to the surface and may even produce some of the exotic chemical species that have been observed in the Io ion torus. A search for transient optical and radio frequency emissions by the Galileo spacecraft may permit the identification and study of discharge phenomena on Io, if they are large enough to be detected. Such a search should concentrate on the equatorial region at night. The discharges are likely to be the most frequent and intense in this region of the satellite because it is exposed to the highest flux of energetic particles (*4, 13*); at night we expect that the electrical conductivity of the surface will be lower because of the lower temperatures. A change in the electrical conductivity of materials generally occurs as a result of prolonged exposure to a radiation environment such as that of Io [(*2*) and references therein]. If the conductivity increases, weaker and less frequent discharges could occur on older sulfur flows. Of critical importance for the detection and consequences of discharges on Io are the spatial dimensions of each discharge and their energy and frequency. Because we have a reasonably detailed picture of Io's environment, the laboratory simulations of the range of conditions expected may provide a rough estimate of the strength, frequency, and spatial scale of discharges on Io.

The surface discharges we are proposing for Io are fundamentally different from the electric arcs that have been suggested by Gold (*14*). Surface discharges will occur preferentially where the temperature is lowest, whereas arcs, such as those proposed by Gold, would be confined to the vicinity of the hot spots where eruptions occur.

More generally, we expect that surface discharges will occur in almost every environment where a suitable dielectric is exposed to large fluxes of energetic particles. Surface discharges could play a role in the synthesis of biogenic compounds and could modify the composition, texture, and optical properties of surfaces. The key questions are whether the discharges occur frequently enough and with enough energy to be significant. In the solar system, the most likely sites will be within the magnetospheres of the giant planets, including the satellites and rings of Jupiter, Saturn, and Uranus. Other locations could be the lunar surface during crossings of the earth's magnetotail, and the surfaces of some asteroids and inactive comet nuclei during solar flares. Surface discharges may also play a role in circumstellar dust shells exposed to energetic outflows of ionized gas from young stellar objects; therefore, surface discharges might have been an important process during the formation of our solar system.

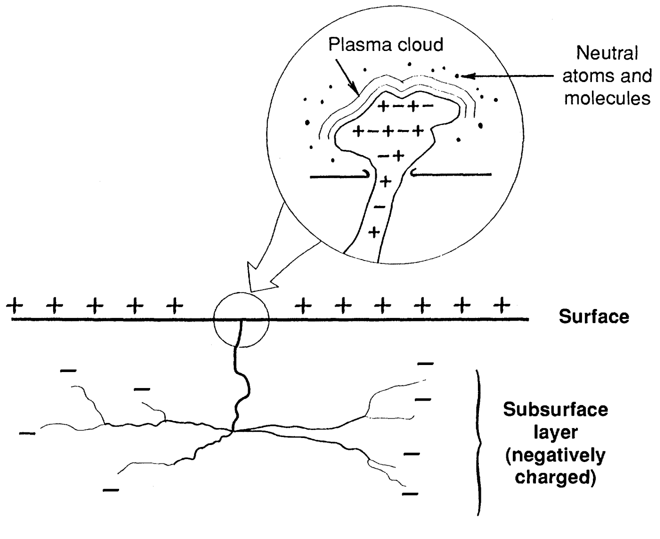

Fig. 3. A schematic representation of a surface discharge on a dielectric polymer surface (*8*). Where the discharge channel reaches the surface there can be localized melting and boil-off of constituent atoms and molecules as well as the generation of a plasma cloud.

REFERENCES AND NOTES

1. K. G. Balmain, in proceedings of the *AGARD Conference (No. 406) on the Aerospace Environment at High Altitudes and Its Implications for Spacecraft Charging and Communications*, The Hague, Netherlands, 2 to 6 June 1986 (North Atlantic Treaty Organization, Brussels, 1987), pp. 16-1–16-7.
2. A. R. Fredrickson, D. B. Cotts, J. A. Wall, F. C. Bouquet, *Prog. Astronaut. Aeronaut.* **107**, 1 (1987).
3. H. B. Garrett, *ibid.* 71, 167 (1980).
4. D. G. Nash *et al.*, in *Satellites*, J. A. Burns and M. S. Matthews, Eds. (Univ. of Arizona Press, Tucson, 1986), pp. 629–688.
5. A. F. Cheng *et al.*, *ibid.*, pp. 403–436.
6. N. Divine and H. B. Garrett, *J. Geophys. Res.* **88**, 6889 (1983).
7. J. E. Nanevicz, J. S. Thayer, K. L. Hewitt, paper presented at the Conference on the Behavior of Spacecraft Materials in Space, Toulouse, France, 12 to 16 September 1988 (European Space Agency, Noordwijk, Netherlands).
8. A. R. Fredrickson, *IEEE Trans. Electr. Insul.* **18**, 337 (1983).
9. B. R. F. Kendall, *Tech. Rep. AFGL-TR-85-0018/ NASA CP 2359* (National Aeronautics and Space Administration, Washington, DC, 1983).

10. K. G. Balmain, M. Gossland, R. D. Reeves, W. G. Kuller, in proceedings of an *International Symposium on Spacecraft Materials in Space Environment*, Toulouse, France, 8 to 12 June 1982 (European Space Agency, Noordwijk, Netherlands, 1982), pp. 263–268.
11. O. Berolo, *ibid.*, pp. 1–10.
12. J. E. Nanevicz and R. C. Adamo, *Prog. Astronaut. Aeronaut.* 71, 252 (1980).
13. The trailing side of Io experiences a higher flux of low energy electrons and ions than the leading side; however, it is the more energetic particles that are relevant to surface discharges.
14. T. Gold, *Science* **206**, 1071 (1979).
15. We thank J. Nanevicz for helpful discussions and the use of his laboratory at SRI International. We also thank K. Hewitt and J. Thayer for discussions and assistance with the experiments, S. Lee for the sulfur samples, and F. Herbert and S. Croft for discussions. A portion of this work was supported by the National Aeronautics and Space Administration and NSF at the Planetary Science Institute (PSI). PSI is a division of Science Applications International Corporation; this is PSI contribution 271.

3 April 1989; accepted 14 June 1989

Nonequilibrium Molecular Motion in a Hypersonic Shock Wave

G. Pham-Van-Diep, D. Erwin, E. P. Muntz*

Molecular velocities have been measured inside a hypersonic, normal shock wave, where the gas experiences rapid changes in its macroscopic properties. As first hypothesized by Mott-Smith, but never directly observed, the molecular velocity distribution exhibits a qualitatively bimodal character that is derived from the distribution functions on either side of the shock. Quantitatively correct forms of the molecular velocity distribution function in highly nonequilibrium flows can be calculated, by means of the Direct Simulation Monte Carlo technique.

The motion of molecules in systems that are not in equilibrium has attracted attention since the formulation of the Boltzmann equation (*1–3*). A convenient place to find extremely nonequilibrium conditions is the interior of a normal shock wave in a gas, where the macroscopic properties of the gas change dramatically over a few molecular mean free paths (*4*). Within a shock an upstream equilibrium distribution moving at supersonic speeds makes a transition to a downstream, higher temperature equilibrium distribution drifting at subsonic speeds. For hypersonic shocks the wave's thickness, which is the characteristic distance required for the upstream to downstream transition, is typically about five times the molecular mean free path in the undisturbed flow upstream of the shock front. For flows produced in a wind tunnel with a constant total energy (constant stagnation temperature), the upstream static temperature decreases as the flow Mach number (M) increases; as a result, the random molecular motion of the upstream molecules occupies a progressively smaller volume of velocity space. The higher the value of M, the easier it is to observe details of the transition in the molecular motion as the gas adjusts between its upstream and downstream distributions.

Such velocity space simplification provides advantages analogous to the simplification of rotational and vibrational spectra achieved by flow cooling in expanding gas flows (*5*). In the experiments described here velocity space simplification was used to observe the extremely nonequilibrium molecular motion in a $M = 25$ helium shock wave. The flow's upstream static temperature was 1.5 K, and the downstream temperature was 280 K. A qualitatively bimodal molecular velocity distribution function was observed and compared in detail to predictions from both the Direct Simulation Monte Carlo (DSMC) technique developed by Bird (*6*) and the Mott-Smith assumption (*7*) of a simple weighted combination of upstream and downstream equilibrium distributions. Both Bird and K. Nanbu [see discussions in (*3, 6*)] have shown that the assumptions used in implementing the DSMC technique can be made consistent with the assumptions underlying the Boltzmann equation.

In addition to shock waves in low-density gases, shocks in liquids have been studied (*3, 8, 9*), both with the use of the Navier-Stokes equations and molecular dynamics calculations. Temperature, density, and velocity profiles in liquid argon appear to be described successfully by the Navier-Stokes equations for behind-the-shock pressures up to about 30 kbar, as inferred by comparisons to molecular dynamics calculations (*8*). For a pressure of 400 kbar, the molecular dynamics calculation gives a thicker shock than the Navier-Stokes equations. A similar behavior is found in gases for $M > 2$ when DSMC calculations of shock thickness are compared to results from the Navier-Stokes equations. On the basis of a molecular dynamics calculation, the 400-kbar liquid argon shock exhibits a temperature overshoot of the streamwise component of the random molecular motion (*8*) that is qualitatively similar to shock waves in low-density gases. On the other hand, application of the Mott-Smith molecular velocity distribution to a 400-kbar liquid argon shock apparently gives results that do not compare well to the molecular dynamics calculation (*8*). For low-density gases the Mott-Smith distribution describes the molecular motion adequately at $M = 1.59$ (*10*) but not at $M = 25$. In the dilute gas limit, molecular dynamics calculations represent a solution of the Boltzmann equation but are computationally inefficient as compared to the DSMC technique (*3, 6*).

Measurements of the molecular velocity distribution functions in normal shock waves have been reported for $M = 1.59$ in helium (*11*) and $M = 7.18$ in argon (*12*). In each case the distribution functions were observed by measuring the intensity profiles of predominantly Doppler-broadened emission lines excited by an electron beam with a diameter of ~1 mm and an energy of 20 keV as it passed through the shock. Known as the electron beam fluorescence technique, it has been described in detail elsewhere (*13*). Electron beam fluorescence is useful in gases such as helium that cannot conveniently be probed by laser-induced fluorescence techniques. Emission from a short length (≈1 mm) of the stimulated radiation was used in the experiments. Spectral and thus, by means of the Doppler effect, velocity-

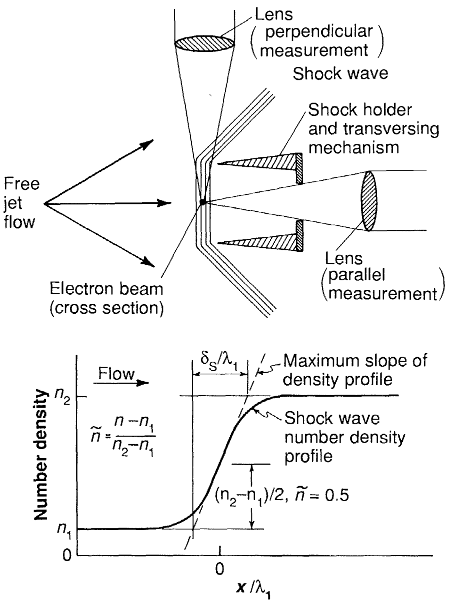

Fig. 1. Experimental arrangement and nomenclature; λ_1, mean free path.

Department of Aerospace Engineering, University of Southern California, Los Angeles, CA 90089.

*To whom correspondence should be addressed.